UC Davis

UC Davis Previously Published Works

Title

Influence of larval behavior on transport and population connectivity in a realistic simulation of the California Current System

Permalink

https://escholarship.org/uc/item/3dh6z28w

Journal

Journal of Marine Research, 71(4)

ISSN

0022-2402

Authors

Drake, Patrick T
Edwards, Christopher A
Morgan, Steven G
et al.

Publication Date

2013-07-01

DOI

10.1357/002224013808877099

Peer reviewed

eScholarship.org Powered by the California Digital Library
University of California

Journal of Marine Research, 71, 317–350, 2013

Influence of larval behavior on transport and population connectivity in a realistic simulation of the California Current System

by Patrick T. Drake[1,2], Christopher A. Edwards[1], Steven G. Morgan[3,4] and Edward P. Dever[5]

ABSTRACT

Using an implementation of the Region Ocean Modeling System, we investigate the influence of larval vertical swimming on spring dispersal for nearshore invertebrate species in the California Current System (CCS), with a focus on central California and the Bodega Bay area. Larvae are given a suite of idealized behaviors designed to reveal the importance of the surface boundary layer (SBL) to transport and settlement. Larvae remain near 5 m, 30 m, or transition between these depths using various strategies, including diel vertical migration (DVM) and ontogenetic vertical migration. Some behaviors result in modeled densities qualitatively similar to observed cross-shelf larval distributions. By remaining primarily below the SBL, larvae released from central California are 500 times more likely to be retained within 5 km of the coast at 30 days from release relative to those that stay near surface, and 145 times more likely to settle along the coast within a 30 to 60 day pelagic larval duration. For most behaviors, nearshore retention over time could be approximated as a modified exponential decay process. Vertical swimming also greatly affects alongshore dispersal, with each behavior resulting in a unique structure of alongshore settlement. Maintaining a depth near 30 m increases settlement throughout most of the CCS by at least an order of magnitude relative to passive larvae. Remaining near surface reduces settlement from Pt. Conception to Pt. Arena, but has less of an effect north of Cape Mendocino. Relative to passive larvae, DVM increases settlement in regional "hotspots," but does not greatly alter overall recruitment in the CCS, and ontogenetic vertical migration increases settlement for central California regions south of Bodega Bay.

1. Introduction

The life histories of many intertidal and subtidal marine species include a planktonic stage during which larvae develop in the coastal ocean for weeks or months before returning to adult populations, which are often sessile or sedentary. Larval dispersal and recruitment can

1. Ocean Sciences Department, University of California Santa Cruz, Santa Cruz, California, USA.
2. Corresponding author ***e-mail: pdrake@ucsc.edu***
3. Bodega Marine Laboratory, University of California Davis, Bodega Bay, California, USA.
4. Department of Environmental Science and Policy, University of California Davis, Davis, California, USA.
5. College of Oceanic and Atmospheric Sciences, Oregon State University, Corvallis, Oregon, USA.

© 2013 Patrick T. Drake, Christopher A. Edwards, Steven G. Morgan and Edward P. Dever.

therefore have a profound effect on the structure and dynamics of many nearshore communities, but larval transport and hence the connectedness of most subpopulations is not well known (Warner et al. 2000; Metaxas 2001; Kinlan and Gaines 2003; Largier 2003; Cowen and Sponaugle 2009). At large temporal and spatial scales, the relatively low swimming speeds of most larvae suggest they are advected passively by often chaotic and unpredictable ocean currents (Thorson 1950; Caley et al. 1996; Metaxas 2001). Modest ocean currents can easily transport passive larvae hundreds of kilometers from their home populations in just a few weeks (Cowen et al. 2003; Largier 2003; Carr et al. 2008; Petersen et al. 2010; Drake et al. 2011; Kim and Barth 2011), yet populations persist. The apparent paradox indicates larvae have developed mechanisms to stay within or return to natal sites, travel from distant subpopulations by unknown pathways, or are supplied by some combination of these factors (Sponaugle et al. 2002). All three possibilities emphasize the need for a more detailed and comprehensive understanding of larval transport.

Dispersal in coastal upwelling regions is particularly intriguing, as the prevailing near-surface currents characteristic of these regions should transport larvae well offshore and equatorward, reducing recruitment to home populations where upwelling is strong (Parish et al. 1981; Roughgarden et al. 1988). Coastal upwelling results from a surface boundary layer (SBL) divergence, caused either by the coastal boundary condition or local wind-stress curl (Dever et al. 2006). Under upwelling favorable conditions, persistent alongshore wind stress and the Coriolis force drive Ekman transport of near-surface waters, and presumably larvae, away from the coast. Most offshore transport is found within the SBL, which includes both the surface mixed layer and a transition region linking the mixed layer to the interior (Lentz 1992). Typically, a diffuse onshore return flow or reduced offshore flow is found at depth. This characteristic upwelling pattern of cross-shore flow has been well-documented throughout the California Current System (CCS) (Checkley and Barth 2009) along the U.S. west coast (Lentz 1987; Kosro 1987; Winant et al. 1987; Lentz 1992; Dever 1997a; Drake et al. 2005; Dever et al. 2006).

Researchers have suggested a variety of mechanisms that would allow larvae to settle given the predominant near-surface offshore flow. Some larvae may be able to return to shore as passive particles during downwelling periods or upwelling relaxation events (Roughgarden et al. 1991; Farrel et al. 1991; Wing et al. 2003; Dudas et al. 2009; Iles et al. 2012). Larval recruitment also may be increased by timing reproduction to occur when offshore transport is reduced (Parish et al. 1981; Shanks and Eckert 2005) and by larvae exploiting opposing, depth-varying cross-shore currents (Peterson 1998; Batchelder et al. 2002; Shanks and Brink 2005).

This latter mechanism has been suggested for northern California in the region immediately north of Pt. Reyes, offshore of Bodega Bay (Wing et al. 1998; Morgan et al. 2009a; Morgan and Fisher 2010; Morgan et al. 2012; Miller and Morgan 2013). The continental shelf between Pt. Reyes and Pt. Arena is an area of persistent wind-driven upwelling, and the physics of the region has been intensively studied (Winant et al. 1987; Largier et al. 1993; Roughan et al. 2006; Halle and Largier 2011). During upwelling favorable winds,

a southward alongshore jet develops over most of the shelf and upper slope (Davis 1985; Kosro 1987; Kaplan et al. 2005; Roughan et al. 2006). The jet separates from the coast at Pt. Reyes (Cervantes and Allen 2006), sometimes forming an offshore-flowing cold filament in satellite images (Strub et al. 1991). When winds relax, a quasi-barotropic poleward-flowing inshore counter-current develops over the inner shelf. Near-surface flow over the shelf in the region is consistently southward and offshore (Winant et al. 1987; Roughan et al. 2006; Halle and Largier 2011) during the spring upwelling season, typically April to June (Strub et al. 1987; García-Reyes and Largier 2012).

Despite the well-documented tendency for offshore flow in the SBL, recent studies have shown that even during strong upwelling conditions, the larvae of many invertebrate nearshore species are found in highest abundance closest to shore, within 10 km of the coast (Wing et al. 1998; Morgan et al. 2009a, 2009b; Morgan and Fisher 2010; Morgan et al. 2012). Additionally, larvae of different species are often found simultaneously in different depth ranges in upwelling regions (Shanks and Brink 2005; Morgan et al. 2009a; Shanks and Shearman 2009; Morgan et al. 2012; Miller and Morgan 2013), implying they are not passive and must be displaying different, species-specific swimming behaviors to retain their depth and cross-shore position. Specifically, during upwelling, larvae can avoid offshore transport by remaining below the SBL.

Modeling studies have shown that larval depth and behaviors that alter it, such as diel vertical migration (DVM, in which larvae reside near-surface at night but at deeper depths during the day) can have a drastic effect on horizontal transport and dispersal in upwelling regions (Batchelder et al. 2002; Marta-Almeida 2006; Peliz et al. 2007; Carr et al. 2008; Petersen et al. 2010; Domingues et al. 2012). Although efforts have been made to assess the importance of larval behavior to dispersal along the western coast of the U.S. (Pfeiffer-Herbert et al. 2007), the effects of behavior on dispersal for nearshore species within the CCS and other areas are often unknown (Metaxas and Saunders 2009; North et al. 2009). In this study, we use an eddy-resolving, numerical model of the CCS to gain quantitative estimates of the effects of several larval behaviors on both transport and dispersal during the spring upwelling season when larvae of many nearshore species are released. Following Pineda et al. (2007), we define larval transport as any movement from one location to another, whereas dispersal is transport between distinct source and settlement sites. And when referring to nearshore species, we include both intertidal and subtidal invertebrates, because observations indicate their larvae employ similar behavioral strategies to realize dispersal in the CCS (Morgan et al. 2009a; Shanks and Shearman 2009). However, as our model does not explicitly include an intertidal zone, it is likely more appropriate for subtidal species.

Our model, an implementation of the Regional Ocean Modeling System (ROMS), was combined with a Lagrangian particle-tracking algorithm in Drake et al. (2011) to give climatological estimates of near-surface, passive larval transport and dispersal in the CCS. Presently, we extend the Drake et al. (2011) study by including previously documented vertical swimming behaviors to determine the importance of transport in the SBL to dispersal.

We concentrate on the central California area surrounding Bodega Bay, where an abundance of historical observations exists. Simulated larvae swim randomly about a fixed target depth, exhibit DVM, perform ontogenetic vertical migration (in which larvae reside near-surface early, but descend to deeper depths later in larval development), or exhibit some combination of these behaviors. The modeled behaviors represent those of many nearshore species in central California with a typical pelagic larval duration of 30 to 60 days (Morgan et al. 2009a; Morgan and Fisher 2010; Shanks and Eckert 2005). Because many of the processes influencing larval dispersal are so poorly constrained (Metaxas 2001; North et al. 2009; Metaxas and Saunders 2009), we concentrate on the interaction of vertical swimming behavior with the Eulerian currents of the CCS, and do not consider other complicating factors for dispersal, such as temperature- or food-dependent growth, mortality and predation or habitat variability. Additionally, due to the relatively long pelagic larval durations (PLDs) of many nearshore species (30 to 60 days, Shanks and Eckert 2005) compared with the near-surface Lagrangian integral time scale of the CCS (two to seven days, Swenson and Niiler 1996), most larvae will likely encounter multiple oceanographic features, locations and ocean states. We therefore analyze the transport from a climatological, probabilistic standpoint, and do not investigate specific trajectories or settlement events.

2. Eulerian model and Lagrangian particle tracking

a. ROMS

Eulerian currents of the CCS were estimated with a configuration of the Regional Ocean Modeling System (ROMS), a terrain-following, primitive equation model (Song and Haidvogel 1994; Shchepetkin and McWilliams 2005). The implementation was described in detail and evaluated in Drake et al. (2011). The model was run continuously for seven years, from January 2000 to December 2006, but here we only consider spring release months (April to June). Briefly, the model employs a 1/30 degree spatial resolution (2.5 to 3.7 km) and 42 vertical levels in a s-coordinate scheme. The domain covered most of the U.S. portion of the CCS (Figure 1). The model was forced at the surface by daily-averaged fields from the Coupled Atmospheric Mesoscale Prediction System (COAMPS) (Hodur 1997; Hodur et al. 2002), specifically 10 m wind velocity, surface air pressure, surface air temperature, shortwave radiation flux, longwave radiation flux, rainfall rate and surface relative humidity. Lateral boundary conditions were provided from monthly climatology taken from the National Oceanographic Data Center World Ocean Atlas (WOA05) (Antonov et al. 2006; Locarnini et al. 2006; Collier and Durack 2006). Subgridscale vertical mixing was accomplished with the Generic Length Scale (GLS) turbulence closure scheme (Umlauf and Burchard 2003), using k-ω parameters (e.g., Warner et al. 2005).

Seasonal surface eddy kinetic energy maps from the model were well-correlated spatially with maps of real, climatological drifter energy derived from Global Drifter Program (GDP) data (Hansen and Poulain 1996) during summer and fall when the eddy field of the CCS

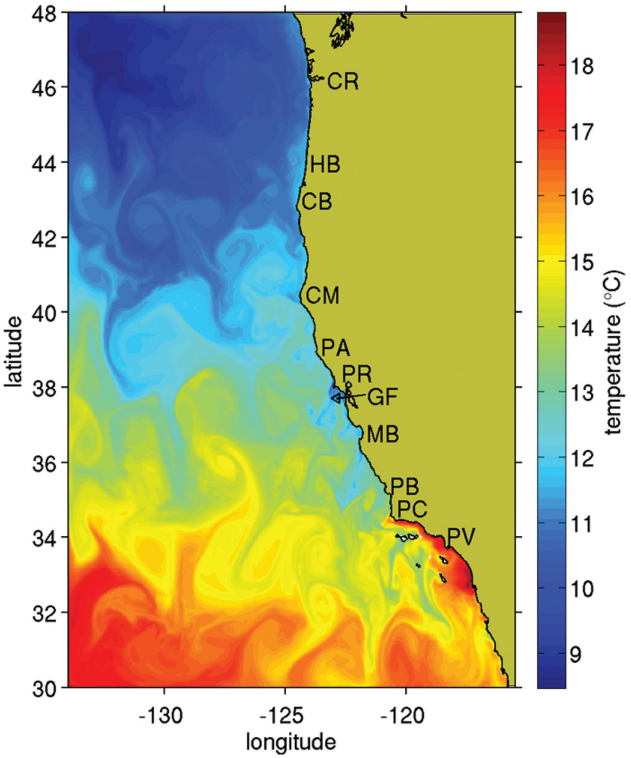

Figure 1. Model domain showing modeled surface temperature (°C) on May 15, 2000. Relevant sites are, from south to north, Palos Verdes (PV), Pt. Conception (PC), Pt. Buchon (PB), Monterey Bay (MB), Gulf of the Farallones (GF), Pt. Reyes (PR), Pt. Arena (PA), Cape Blanco (CB), Heceta Bank (HB) and the Columbia River (CR).

was most energetic (Drake et al. 2011). In addition, seasonal maps of near-surface Eulerian velocities from the model were qualitatively similar to pseudo-Eulerian maps from the GDP drifters.

Here we include a model-data comparison (Table 1) in the Bodega Bay region, which is the principal focus area of our study, using measured ADCP velocities from the D90 mooring of the WEST study (Dever et al. 2006). The D90 mooring was located over the mid-shelf, near the primary larval release site offshore of Bodega Bay (Figure 2). The mooring water depth was 88 and 90 m in the model and observations, respectively. Statistics cover a relevant 90-day period when data was available, May 4 to Aug. 1, 2001. Alongshore and cross-shore directions were determined from the principal axes of the depth-averaged (5 to 77 m) currents (Kundu and Allen 1976). A linear trend was removed from the all time series before calculating r^2 values. To account for temporal autocorrelations, the effective degrees of freedom for correlation significance levels was determined using the integral

Table 1. Modeled and measured current statistics at the WEST study D90 mooring.

Alongshore						
depth range	mean obs.	mean model	std. obs.	std. model	r^2	N^*
5–15 m	−1.6	−3.8	11.5	16.1	0.55	26
25–35 m	−0.1	1.2	11.2	12.3	0.61	29
5–77 m	0.2	1.7	10.2	11.2	0.67	32
Cross-shore						
depth range	mean obs.	mean model	std. obs.	std. model	r^2	N^*
5–15 m	−2.9	−3.5	3.3	4.3	0.31	69
25–35 m	−0.1	0.5	2.3	2.7	n/s	76
5–77 m	−0.5	−0.3	1.4	2.1	n/s	46

Means and standard deviations (std.) are in cm s^{-1}. N^*: effective degrees of freedom for correlation significance levels. The (alongshore, cross-shore) directions are (335°, 65°) and (340°, 70°) in the observations (obs.) and model, respectively (i.e., positive poleward and onshore). All listed zero-lag, squared correlation coefficients (r^2) were different from zero at a significance level of $p < 0.01$. n/s indicates correlations were not significant. All compass directions here and throughout are relative to true north.

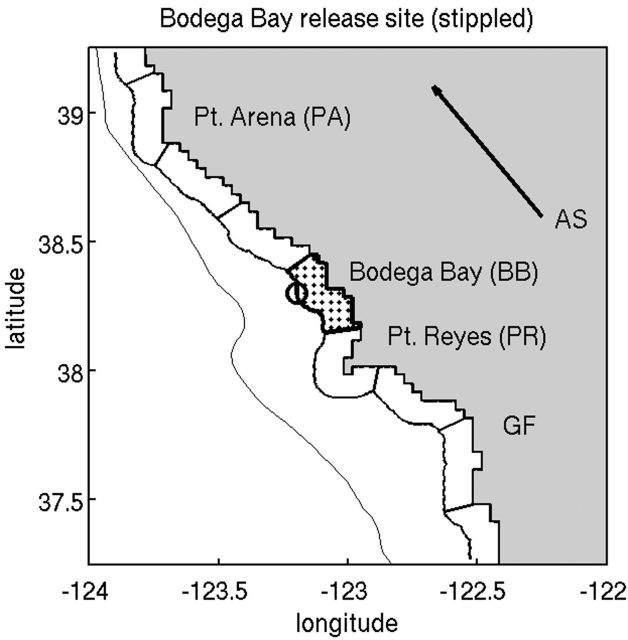

Figure 2. Close up of model coastline showing central California. "Boxes" show larval source and settlement cells, each extending 10 km offshore. The stippled box is the Bodega Bay source cell. The circle indicates the location of the D90 mooring (water depth of 88 m) from the WEST study. Fine black line is the model 250 m isobath. "GF" indicates the Gulf of the Farallones. Arrow indicates positive alongshore (AS) direction (327°) used for alongshore dispersal (Figure 10). All compass directions here and throughout are relative to true north.

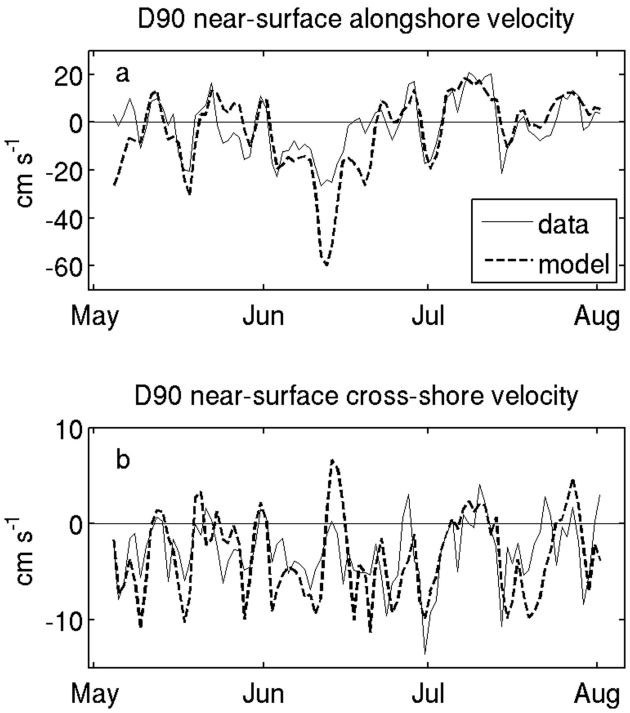

Figure 3. Daily-averaged, near-surface (5 to 15 m) alongshore (a) and cross-shore (b) currents at the D90 mooring during May to July of 2001, shown with different vertical scales. Positive velocities indicate poleward and onshore flow for the alongshore and cross-shore directions, respectively. Zero-lag, squared correlation coefficient (r^2) values were 0.55 and 0.31 for the alongshore and cross-shore directions, respectively (see Table 1 for additional statistics).

time scale, as suggested by Emery and Thompson (1997, Chapter 3) (i.e., $N^* = T/\tau$, where T is the analysis period, and τ is the integral time scale). The longest integral time scale of either the observations or model was used in the previous equation, yielding the most conservative (i.e., smallest) of the two available estimates of N^*. ADCP depth bins at 8 and 36 m were potentially contaminated by reflections from other instruments and not considered.

Model alongshore currents agreed well with daily-averaged, moored velocity measurements. Near-surface (5 to 15 m) currents from the model were significantly correlated with measured ADCP velocities, in both the alongshore and cross-shore directions (Table 1 and Figure 3). In addition, depth-averaged (5 to 77 m) and subsurface (25 to 35 m) alongshore currents were well correlated between the model and data. But depth-averaged, cross-shore fluctuations did not agree, nor did cross-shore velocities at mid-depth (Table 1). In both the model and data, mean cross-shore velocity profiles displayed a classic upwelling structure

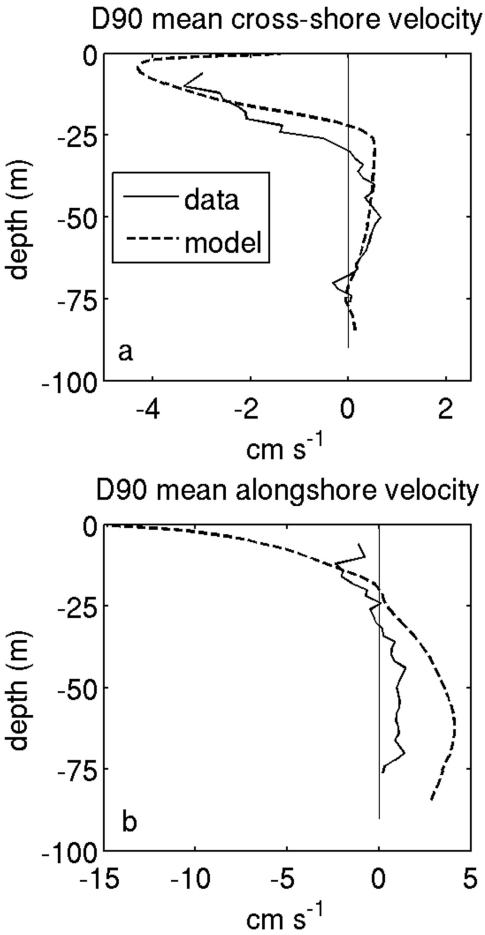

Figure 4. Cross-shore (a) and alongshore (b) time-average velocity profiles at the D90 mooring for May to July of 2001, shown with different horizontal scales. Positive velocities indicate onshore and poleward flow for the cross-shore and alongshore directions, respectively.

(Figure 4a), with offshore flow near-surface and onshore flow at depth, as found in previous studies (Lentz 1987). The cross-shore zero-crossing indicates the approximate location of the base of the time-averaged SBL at this location and was located at 23 m in the model and 30 m in the measurements. Mean alongshore currents also displayed a similar vertical structure in the model and data, with equatorward flow near-surface and poleward flow at depth. The model overestimates the near-surface mean and fluctuating velocities, however (Figure 4b and Table 1), and the pronounced vertical shear in the upper 5 m is likely too large.

b. Larval trajectories with vertical swimming

Particle trajectories were calculated using an offline version of the ROMS internal Lagrangian drifter module as described in Drake et al. (2011), here modified to accommodate vertical swimming behavior. The offline Lagrangian module used an hourly time-step and interpolates daily-averaged, Eulerian velocity fields linearly in time and all three spatial dimensions onto particle positions. In the present study, particles were transported horizontally with a Euler-trapezoidal, predictor-corrector scheme employing a single iteration. This scheme is lower order than the backward-looking Milne scheme employed in the previous study, but more appropriate for non-passive larvae. Our virtual, swimming larvae will change their depth by tens of meters over a few hours (i.e., a few Lagrangian time-steps). Hence due to the vertical shear of the CCS, their horizontal velocity can also vary substantially in one time step, making the backward-looking Milne scheme less appropriate.

For all swimming behaviors (see Section 3. Swimming behaviors), virtual larvae were programmed to form a normal vertical distribution about a target depth of either 5 or 30 m. Target depths were updated semi-diurnally; swimming velocities were updated hourly. Swimming speeds were limited by a maximum, but otherwise increased exponentially with distance away from the target depth: $w_l = w_{\max}\ \mathrm{sgn}\ (d - z)(1 - e^{-|d-z|/\lambda})$, where w_l is the swimming velocity of an individual larva, $w_{\max}$ is a maximum swimming speed of 0.005 m s^{-1}, sgn is the sign function, d is the target depth, z is the depth of the larva, and $\lambda = 12$ m. The functional form and parameter values chosen ensured larvae could approximately reach, but not substantially overshoot, their target depths in one time-step. The maximum swimming velocity is within the range of swimming speeds of crustacean larvae in the CCS (Shanks 1985; Shanks 1986; Hobbs and Botsford 1992; Shanks 1995a) and zooplankton aggregations observed elsewhere (Genin et al. 2005). The swimming velocity was added to the ROMS Eulerian velocity, and particles were then moved vertically with a first-order Euler scheme. In addition, a random, normal offset was given to each larva's swimming speed to create a normal vertical distribution about the target depth with standard deviation of 2.5 m.

Where the target depth fell below the sea floor, larvae were reassigned a target depth 2.5 m above the ocean bottom. In practice, this occurred for a substantial number of larvae during the first few weeks of release, as they were released in relatively shallow water over the inner- and mid-shelf. Any larvae attempting to swim below the sea floor (due to the random contribution to the swimming velocity) were reflected off the bottom. Passive larvae were given a zero swimming velocity at all times, but were mixed vertically with a random walk model based on the local vertical turbulent Eulerian diffusivity as described in Drake et al. (2011). However, the passive case investigated here differs slightly from the previous study due to the present use of the Euler-trapezoidal scheme for horizontal motion and addition of simulated tidal mixing.

Larvae programmed to swim below the SBL had a tendency to move onshore. This transport led to a substantial fraction of larvae moving into land areas or accumulating within

a grid point of the coast where horizontal velocities were small. This phenomenon was absent from the previous study, where passive larvae followed the three-dimensional circulation and were not confined by behavior to depths where flow was consistently onshore. To correct this unrealistic effect, onshore motion was disabled in all cases if it resulted in a larva intersecting the coast. Alongshore motion always remained intact, however. Additionally, at each time step when in water depths < 800 m, larvae were given a random normal horizontal displacement simulating tidal mixing. The displacement corresponds to a tidal diffusivity of 25 $m^2\ s^{-1}$, appropriate for tidal velocities on the central California shelf of roughly 0.05 $m\ s^{-1}$ (Kaplan et al. 2005; Rosenfeld et al. 2009; Wang et al. 2009).

c. Larval release and settlement

Particles were released within horizontal release and settlement cells at the coast extending 10 km offshore, each with an area of approximately 400 km^2 (Figure 2). The release is identical to that described in Drake et al. (2011) and ranged from Palos Verdes in southern California to Heceta Bank in central Oregon. Larvae were given an initial random uniform vertical distribution from 0 to 20 m and released every-other-day in April, May and June for seven years, from April 2000 to June 2006. We concentrate on one release cell surrounding Bodega Bay in central California where approximately 150 larvae were released every-other-day.

Climatological probability density functions (pdfs) of larval position at 30 days-since-release were created by averaging the pdfs of all releases, simulating an instantaneous release. Pdfs were normalized such that the integral of larval density over the domain was equal to unity at time of release. If larvae were transported out of the model domain, the integrated density decreased. However, this loss amounted to less than 0.01 of released larvae at 30 days-since-release for all cases. The pdfs employed a spatial resolution of 100 km^2 for horizontal (10 km $\times$ 10 km bins), 5 km for distance-from-shore, and 1 m for vertical distributions. Distance-from-shore was determined by the shortest absolute distance to any point on the model coastline. Each pdf from Bodega Bay consists of over 46,400 larvae. The total number of larvae released in other cells ranged from 20,000 to 70,000, due to the variability of the coastline.

To calculate settlement, larvae were assumed to settle if found within a settlement cell (same as release cells, see Figure 2) during a larval competency window of 30 to 60 days-since-release. Larvae could not settle to the Channel Islands or estuaries such as San Francisco Bay, but otherwise habitat availability is not considered. Because we do not include post-settlement mortality, dispersal between sites also represents the pre-reproductive population connectivity of potential subpopulations (Pineda et al. 2007). We define connectivity quantitatively as the matrix $C(x, y)$ giving the fraction of larvae released from coastal cell x that settle to coastal cell y. Each connectivity matrix consists of over 1.6 million released larvae.

3. Swimming behaviors

It has been proposed that larvae can control, or at least heavily influence, cross-shore and horizontal transport by regulating depth (Paris and Cowen 2004; Queiroga and Blanton 2005; Shanks and Brink 2005; Marta-Almeida et al. 2006; Naylor 2006; Morgan et al. 2009a; Shanks and Shearman 2009; Domingues et al. 2012). However, the exact mechanisms and cues used by larvae to maneuver and swim vertically are often unknown, as is the ultimate importance of larval behavior to dispersal (Metaxas 2001; Metaxas and Saunders 2009). Further in this paper we describe six distinct behaviors used in the present study, in addition to the null hypothesis of no behavior (i.e., passive particles). The idealized modeled behaviors approximate real behaviors inferred from observed larval densities in the CCS and laboratory (Peterson 1998; Pfeiffer-Herbert et al. 2007; Morgan et al. 2009a; Shanks and Shearman 2009; Morgan et al. 2012; Miller and Morgan 2013). They are designed to illustrate the importance of the SBL and its associated wind-driven currents to larval transport and dispersal.

Specifically, modeled larvae are given a random, normal vertical distribution about time-changing target depths (Table 2). The choice of target depth enables larvae to remain within the SBL throughout development, swim below this layer throughout development, or exhibit some temporal combination of these two states. As discussed by Shanks and Brink (2005), it is the position of the larvae in the water column relative to the SBL, not their absolute depth that determines the effects of upwelling or downwelling. We recognize that at any given time and location larvae displaying a particular modeled behavior may or may not be in the SBL. However, sensitivity studies revealed that the effective, climatological offshore Lagrangian transport in the model was confined to a surface layer with a depth of approximately 20 m. Therefore, when discussing behaviors, we relate the larvae to a fixed, idealized SBL depth of 20 m for conceptual and semantic convenience. In all behavioral cases, larval vertical distributions are given a standard deviation of 2.5 m. This random displacement ensures 95% of the larvae are confined to a 10 m thick layer that can be classified as either predominantly in or below the SBL, at least in a climatological sense.

Our modeled behaviors are inspired by similar behaviors in nature that are believed to accomplish a variety of different transport outcomes. The passive case will sweep many larvae offshore during spring (Drake et al. 2011), but may allow some larvae to be downwelled and remain nearshore. The in-SBL behavior (i.e., in surface boundary layer) will likely transport larvae offshore and southward. The below-SBL case may retain larvae nearshore and encourage northward transport. The DVM behavior should help reduce offshore and southward transport, as well as decrease fish predation. The ontogenetic case may allow larvae to return to shore at depth after a development period over the shelf. The reverse-ontogenetic behavior may be employed by larvae that concentrate in the neuston later in development, where surface and internal waves (not modeled here) and onshore winds may bring them back to the coast. Larvae exhibiting the ontogenetic-DVM behavior may initially migrate to the outer half of the continental shelf before returning to shore at

Table 2. Description of modeled behaviors.

Behavior Name	Target Depth and Swimming Rules	Potentially Relevant Species in the Bodega Bay Area
passive	larvae move passively with ambient vertical currents and are mixed vertically by ambient turbulence	unknown
in-SBL	larvae stay near 5 m, within the surface boundary layer (SBL)	Most *Cancer* crabs (*C. magister*, *C productus, C. oregonensis*) and spider crabs (Majidae)
below-SBL	larvae stay near 30 m, below the SBL	Most barnacles (*Balanus crenatus*, *Semibalanus cariosus* and *Chthamalus* spp.)
DVM	larvae undergo diel vertical migration (DVM) from 30 m during the day to 5 m at night, with equal time at each depth	crabs, except pea crabs (Pinnotheridae)
ontogenetic	Larvae stay near 5 m for an initial 9 days, then descend to 30 m for the remainder of their pelagic larval duration (PLD)	pea crabs (Pinnotheridae)
reverse-ontogenetic	larvae remain near 30 m for an initial 21 days, then ascend to 5 m for the remainder of their PLD	barnacle *(Balanus glanduIa)*
ontogenetic-DVM	larvae remain near 5 m for an initial 9 days, then migrate daily from 30 m to 5 m for the remainder of their PLD	hermit crabs (*Pagurus* spp.), rock crab (*Cancer antennarius*), and graspid crabs

Behaviors were implied by observed larval densities of benthic crustaceans off Bodega Bay, California (Morgan et al. 2009a; Morgan and Fisher 2010; Morgan et al. 2012). In all behavioral cases, larvae are given a random, normal vertical distribution with standard deviation of 2.5 m about a potentially time-varying target depth (5 or 30 m). The random distribution is updated every Lagrangian time step (hourly).

depth, while undertaking DVM near the end of development to avoid fish predation. In this case, DVM is not expressed during the early larval phase while larvae expedite offshore transport by remaining in the SBL.

The modeled behaviors provide a sound starting point to quantify the bulk effects of vertical position on horizontal larval transport within the CCS. Although inspired by ecological rationales, the behaviors are idealized and not intended to mimic the precise behavior of any particular species. The modeled layer thickness (standard deviation of 2.5 m) is roughly consistent with existing observations of larval distributions (Morgan et al. 2009a; Shanks and Shearman 2009; Morgan et al. 2012). However, these measurements were taken with relatively low vertical and temporal resolution (two to four daily transects with three to five stratified samples taken at each station). Higher-resolution acoustic measurements in the

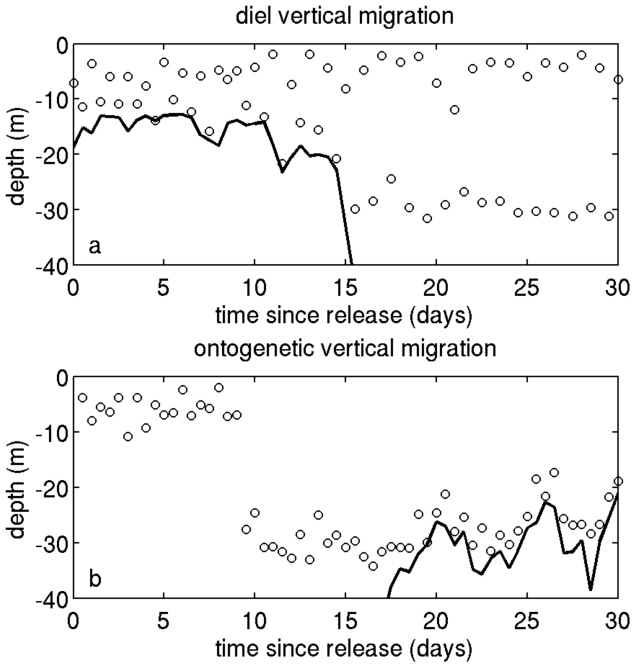

Figure 5. Vertical trajectory (circles) of a single Bodega Bay larva given the (a) DVM and (b) ontogenetic behaviors. Heavy black curve is the local water depth at the larva's horizontal location (i.e., the ocean bottom).

nearshore CCS indicate larvae and other zooplankton frequently aggregate in evanescent layers typically less than a few meters thick (McManus et al. 2005; Cheriton et al. 2007; Benoit-Bird 2009). The behaviors are non-interactive and do not adjust to the changing pycnocline, current shear, turbulent kinetic energy or prey availability, factors known to influence many real species (Metaxas 2001; Metaxas and Saunders 2009). As variations in larval vertical density are likely correlated with horizontal current velocities, our idealized behaviors may bias the eventual horizontal transport results.

Larval behaviors often interacted with the local bathymetry (Figure 5). For example, the initial DVM of one selected larva is limited by the ocean bottom for the first 15 days of its PLD (Figure 5a). As it moves into deeper water, however, it is able to descend to its daytime target depth of 30 m. Larvae displaying the ontonogenic behavior were often limited by the local water depth later in their PLD (Figure 5b), as onshore currents at depth moved them shoreward. For the in-SBL behavior, however, larvae rarely interacted with the bottom and are distributed approximately normally about 5 m as intended (Figure 6). In contrast, the distribution of below-SBL larvae is not unimodal (Figure 6), as many larvae are in water shallower than 30 m and are unable to reach their target depth. A similar but smaller secondary peak is also present in the ontogenetic distribution (Figure 6). In this instance,

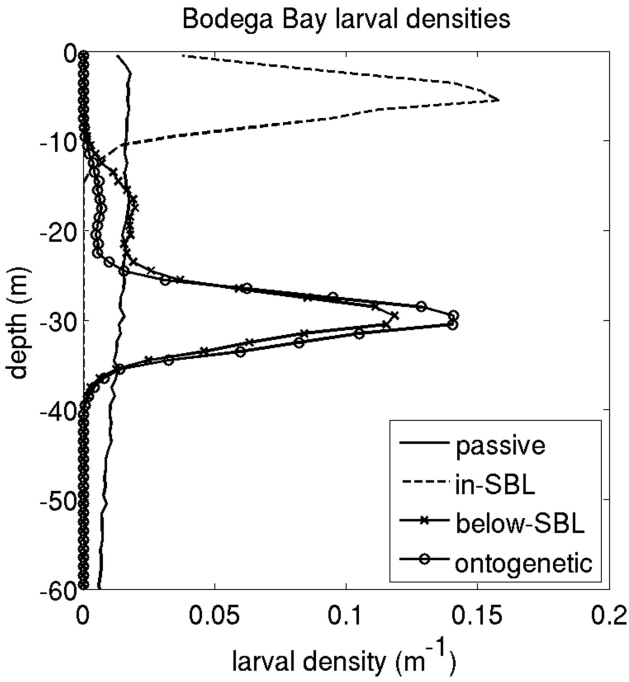

Figure 6. Vertical distribution (probability density function) of larvae from the Bodega Bay release area at 30 days-since-release given a variety of behaviors. These curves represent the superposition of larvae over the entire domain, and local vertical distributions may differ. The secondary peak surrounding −16 m for the below-SBL and ontogenetic cases (circles and crosses) represents larvae attempting to reach 30 m depth, but constrained by a shallower local water depth.

larvae move offshore during the first nine days of development when they are in the SBL. Virtually all larvae then descend to 30 m, where currents are more shoreward and a small fraction of larvae begin to migrate back onshore, some into depths less than 20 m. Passive particles exhibit a relatively broad distribution (Figure 6).

4. Central California surface boundary layer, transport and nearshore retention

a. Surface boundary layer

The surface boundary over the central California shelf is highly spatially and temporally variable (Lentz 1992; Dever et al. 2006). It generally increases with water depth out to the shelf break and with wind stress overall. Modeled Lagrangian transport from Bodega Bay releases displayed a clear relationship to this layer, with deeper swimming depths always leading to more retention nearshore over a broad range of target depths investigated, 5 to 80 m (not shown). This sensitivity to target depth was most pronounced near 15 m. Larvae swimming consistently at a depth of approximately 20 m were more likely to be

retained within 20 km of the coastline at 30 days-since-release than those swimming slightly shallower, about 10 m, by a factor of 25. This ratio indicates substantial vertical shear in the mean cross-shore velocity between 10 and 20 m over the shelf and slope for our model implementation. It also implies an effective layer of intense offshore transport extending from the surface to ~20 m. This depth is shallower than the base of offshore flow found at the D90 mooring (23 and 30 m in the model and observations, respectively (Figure 4)). It is also shallower than the base of similar Eulerian layers found by Lentz (1987) (15 to 35 m) and Kosro (1987) (20 to 50 m) for the area and season, but is slightly deeper than the mean surface mixed layer depth found by Lentz (1992) (10 m). This depth comparison is intended illustratively and for completeness. The Lagrangian transport represents the integral of the instantaneous current at a variety of times and locations along the larval trajectories, and in general cannot be predicted from the Eulerian mean flow (Davis 1991).

b. Transport and nearshore retention

Depth-integrated larval densities for Bodega Bay larvae at 30-days-since-release ranged widely among behaviors (Figure 7). Over the shelf near Bodega Bay, larval densities are highest for the below-SBL larvae and lowest (almost nonexistent) for the in-SBL behavior. Most in-SBL larvae have moved far offshore and south of Gulf of the Farallones, entirely out of the greater release region. The same is true for the ontogenetic-DVM case (not shown), whose density map is intermediate between the DVM and in-SBL cases. The remaining cases show some retention near Bodega Bay, but the density is at least a factor of three higher for the below-SBL case, implying that swimming below the SBL may be critical for local settlement. A large difference exists in alongshore density between the below-SBL and reverse-ontogenetic cases, demonstrating that just nine days spent in the SBL (reverse-ontogenetic case) can radically alter net alongshore transport. Northward transport for the below-SBL, ontogenetic and reverse-ontogenetic cases is limited to just north of Pt. Arena and is negligible for all other cases, reflecting the predominantly southward flowing near-surface currents of the CCS. The densities of the ontogenetic, reverse-ontogenetic, passive and DVM behaviors are similar in that most larvae retained over the shelf and upper slope are south of Pt. Reyes in the Gulf of the Farallones or Monterey Bay areas, rather than near the release location.

The effects of behavior on nearshore retention of Bodega Bay larvae can be seen more clearly when the larval density is integrated over the alongshore direction (Figure 8). Immediately at the coast (0 to 5 km from shore), densities of different behaviors span more than two orders of magnitude, with the below-SBL density being 500 times greater than the in-SBL case. If the density is summed over the first 20 km from shore, the factor reduces to 120. Unscaled densities (not shown) are maximal immediately at the coast only for the below-SBL and ontogenetic behaviors. All other cases display a minimum in unscaled density at the coast, with densities increasing gradually offshore to a maximum at 50 to 150 km from shore.

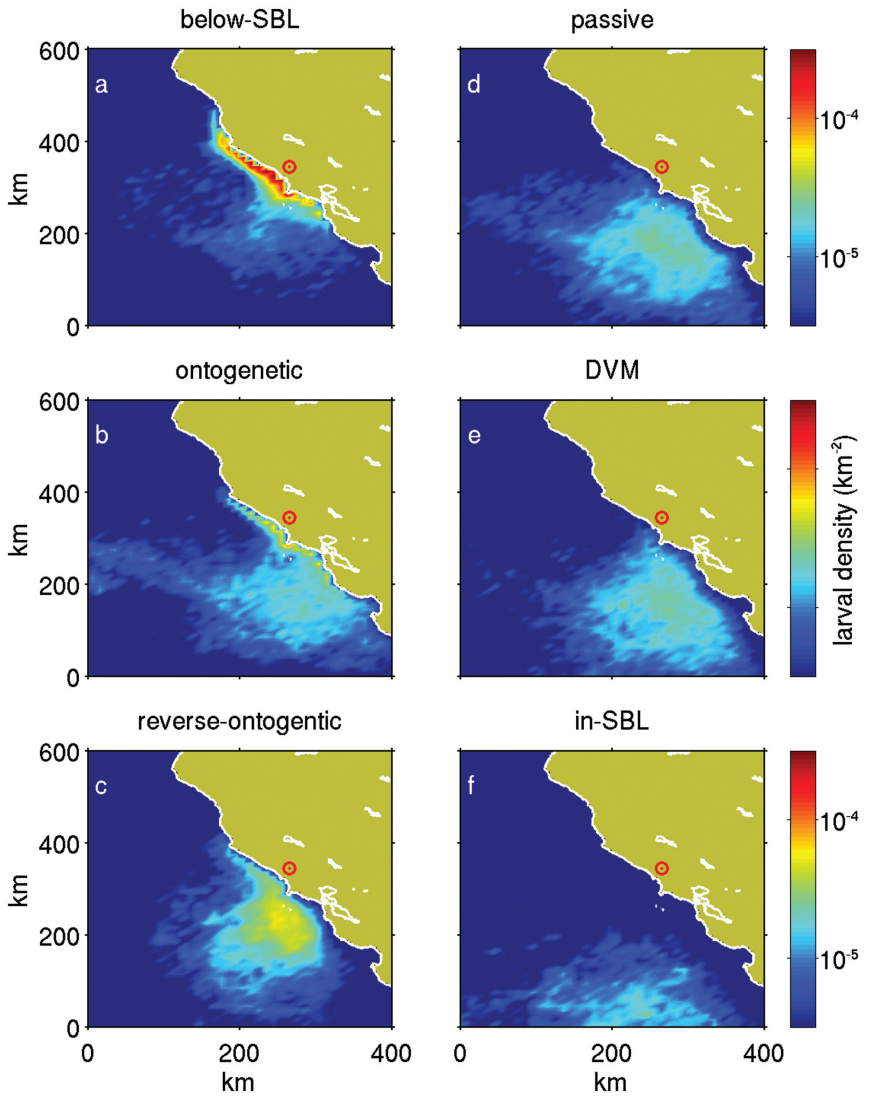

Figure 7. Two-dimensional larval density at 30 days-since-release for Bodega Bay area larvae given a variety of behaviors, shown with a log_{10} color scale. Red circle is a land area adjacent to release cell (Figure 2). The units are fraction of total released found per km^2. The model did not contain and larvae could not enter San Francisco Bay.

With the exception of the ontogenetic and reverse-ontogenetic behaviors, the coastal densities (i.e., the fraction remaining within 10 km of shore at 30 days-since-release) can be rank ordered simply by the number of days the larvae have spent above 20 m, with more time spent near-surface leading to less nearshore retention (Table 3). Time in the SBL was

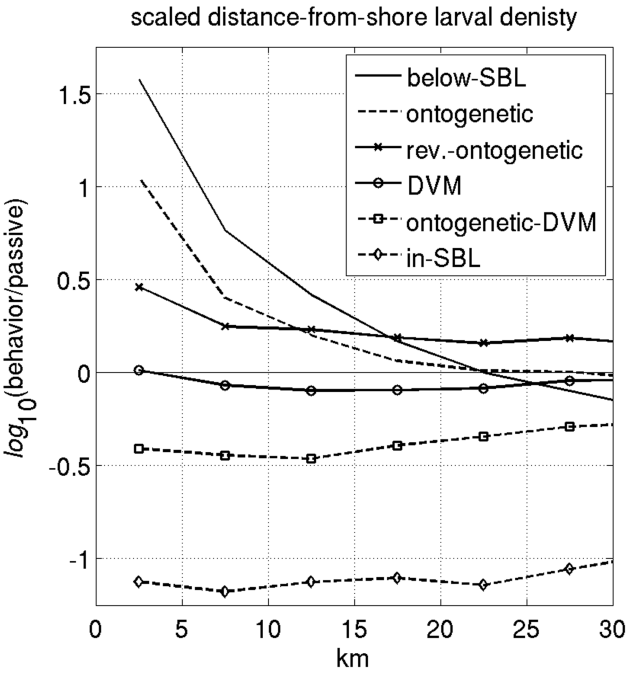

Figure 8. Scaled larval density as a function of absolute distance-from-shore for Bodega Bay area larvae at 30 days-since-release. Densities for a variety of behaviors are scaled by the passive larval density and plotted with a log_{10} vertical scale (i.e., $log_{10}(\rho_{\text{behavior}}/\rho_{\text{passive}})$, where ρ is the one-dimensional density). With this scaling, values above and below the x-axis represent densities greater and less than the passive case, respectively.

Table 3. Fraction of Bodega Bay area larvae from a spring release remaining within 10 km of shore at 30 days-since-release for a variety of behaviors.

Behavior	Time in SBL (Days)	Fraction Within 10 km of Shore
below-SBL	0	0.54
ontogenetic	9.0	0.17
reverse-ontogenetic	9.0	0.063
passive	13	0.028
DVM	15	0.026
ontogenetic-DVM	20	0.010
in-SBL	30	0.0020

estimated from the larvae's nominal (i.e., target) depths, except for the passive case where the statistic was calculated directly from individual trajectories. Although ontogenetic and reverse-ontogenetic larvae spend the same amount of time in the SBL (nine days), the ontogenetic density is almost three times the reverse-ontogenetic value. At 30 days-since-release,

Table 4. Fraction of Bodega Bay area ontogenetic larvae from a spring release remaining within 10 km of shore, as a function of time-since-release. Ontogenetic larvae descend from 5 to 30 m depth at 9 days-since-release.

Time-Since-Release (Days)	Fraction Within 10 km of Shore
0	1.0
5	0.29
10	0.12
15	0.14
20	0.16
25	0.17
30	0.17

the ontogenetic larvae have been below the SBL for the previous 21 days, and many of the larvae that were swept offshore initially have returned to the inner shelf (Table 4). This behavior is the only one investigated exhibiting an increase in nearshore density with time, and it represents both a vertical and cross-shore migration (Peterson 1998; Morgan et al. 2009a). The opportunity for ontogenetic larvae to return to shore at depth after offshore transport near-surface is the cause of the difference in ontogenetic and reverse-ontogenetic densities.

With the exception of the ontogenetic case, the relationship between time spent in the SBL and the fraction remaining nearshore can be well-modeled empirically as the product of two decaying exponentials: $F(t_1, t_2) = \exp(-t_1/\tau_1)\exp(-t_2/\tau_2)$, where F is the fraction remaining within 10 km of the coastline, t_1 is time spent below the SBL, t_2 is time spent in the SBL, and τ_1 and τ_2 are constants to be determined. The model is reasonable over $0 \leq (t_1, t_2) \leq 30$ days and has been evaluated for the Bodega Bay release cell only. Nearshore densities are well modeled with $\tau_1 = 50$ days and $\tau_2 = 4.0$ days (Figure 9). Values of (τ_1, τ_2) were determined by finding the best fit in the least squares sense for the below-SBL and in-SBL cases, respectively. This empirical model implies a climatological spring-time half-life for larvae in the SBL over the central California inner-shelf of 2.8 days.

The functional form of F suggests the offshore loss of larvae can be understood as a product of two processes. The first process results in a relatively slow loss that occurs when the larvae are below the SBL. The second process is a much faster decay that operates when the larvae are within the SBL and dominates changes in F for most behaviors. This dominant loss can be explained by envisioning a well-mixed box of larvae residing in the nearshore SBL that is experiencing both upwelling and offshore Ekman transport. Larval-free upwelled waters enter the box from below, entrain larvae, and are then exported offshore. The offshore larval loss in a given time, dt, is then $dF = -vF/\Delta x dt$, where v if the effective offshore velocity (here positive offshore) and Δx is the cross-shore width of the box. The solution of the above differential equation is $F = \exp(-vt/\Delta x)$, implying $v = \Delta x/\tau_2$. Given $\Delta x = 10$ km and $\tau_2 = 4.0$ days, the preceding equation yields $v = 2.9$ cm s^{-1}. In

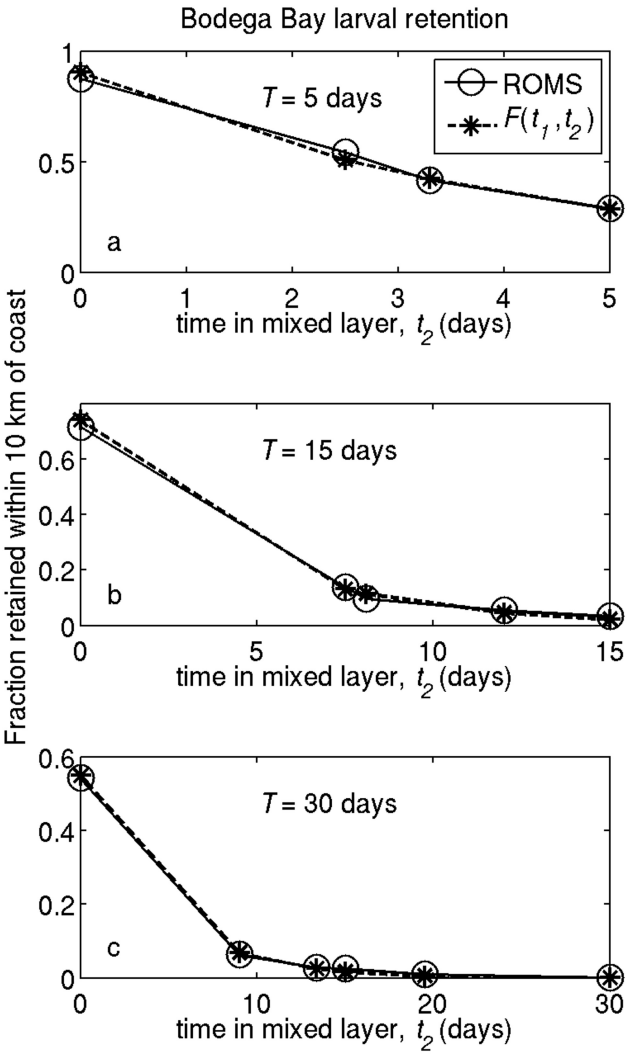

Figure 9. Fraction of Bodega Bay larvae remaining nearshore as a function of both time spent below the SBL (t_1) and time in the SBL (t_2), calculated from the ROMS model (circles) and estimated using the empirical analytical function $F(t_1, t_2) = \exp(t_1/\tau_1)\exp(t_2/\tau_2)$ (stars), where F is the fraction remaining within 10 km of shore, $\tau_1 = 50$ days and $\tau_2 = 4.0$ days. Each (x, y) point represents the retention of a different behavior with specific (t_1, t_2). Panels a, b and c correspond to time-since-release, $T = 5$, 15 and 30 days, respectively, and $T = t_1 + t_2$.

comparison, the time-mean cross-shore velocity in the ROMS model at the D90 mooring (near the offshore edge of the box) when calculated over all seven springs (April to July) at 5 m depth was 3.1 cm s^{-1}, suggesting the above box model is physically reasonable. This single-point velocity comparison is only intended illustratively, however, as the effective

Table 5. Settlement statistics given a spring release and 30 to 60 day competency window for all behaviors.

	All Release Cells	Bodega Bay Release Cell		
Behavior	*S*	*S*	<PLD> (days)	time in SBL (days)
below-SBL	0.65	0.64	32	0
ontogenetic	0.33	0.30	35	9
reverse-ontogenetic	0.17	0.096	32	11
passive	0.084	0.094	38	13
DVM	0.092	0.063	36	18
ontogenetic-DVM	0.066	0.031	37	23
in-SBL	0.026	0.0044	33	33

S: settlement strength, or fraction of larvae released that eventually settle; <PLD>: mean realized pelagic larval duration of settling larvae; time in SBL: mean time settling larvae spend in the surface boundary layer.

velocity, v, is in general a combination of the Eulerian velocity weighted by the larval density at all relevant depths, locations and times.

5. Behavior and dispersal

a. Dispersal from central California

Vertical swimming behavior greatly affected modeled spring-time dispersal. The effect can be quantified with the overall settlement strength S (the total fraction of those released that eventually settle). Settlement strength from the Bodega Bay cell follows the rank ordering of behaviors found for the nearshore retention statistic (Table 5, compare with Table 3). Settlement is greatest for the below-SBL and ontogenetic larvae, which are at depth during the competency window. Settlement for the in-SBL and ontogenetic-DVM behaviors, which keep larvae predominantly in the SBL is weakest, as suggested by the nearshore retention results above. But settlement strengths for reverse-ontogenetic and passive cases are nearly identical, and they differ from the retention results where densities of passive larvae were twofold lower than the reverse-ontogenetic case. The relative increase in settlement strength for the passive behavior is the result of southward dispersal of passive larvae absent from the reverse-ontogenetic case.

The average larval age at settlement, or realized mean PLD (<PLD>, where $< \cdot >$ indicates a mean over all settling larvae), varied with behavior, with passive larvae displaying the greatest <PLD> and both the below-SBL and reverse-ontogenetic behaviors the least (Table 5). Settlement strength decreased monotonically with average time spent in the SBL, but it was not a monotonic function of <PLD> (Table 5).

The behaviors resulted in complex patterns of alongshore dispersal for Bodega Bay larvae, with each behavior displaying unique structure (Figure 10). Passive larvae display a broad area of substantial settlement from 300 km south to 100 km north of Bodega Bay

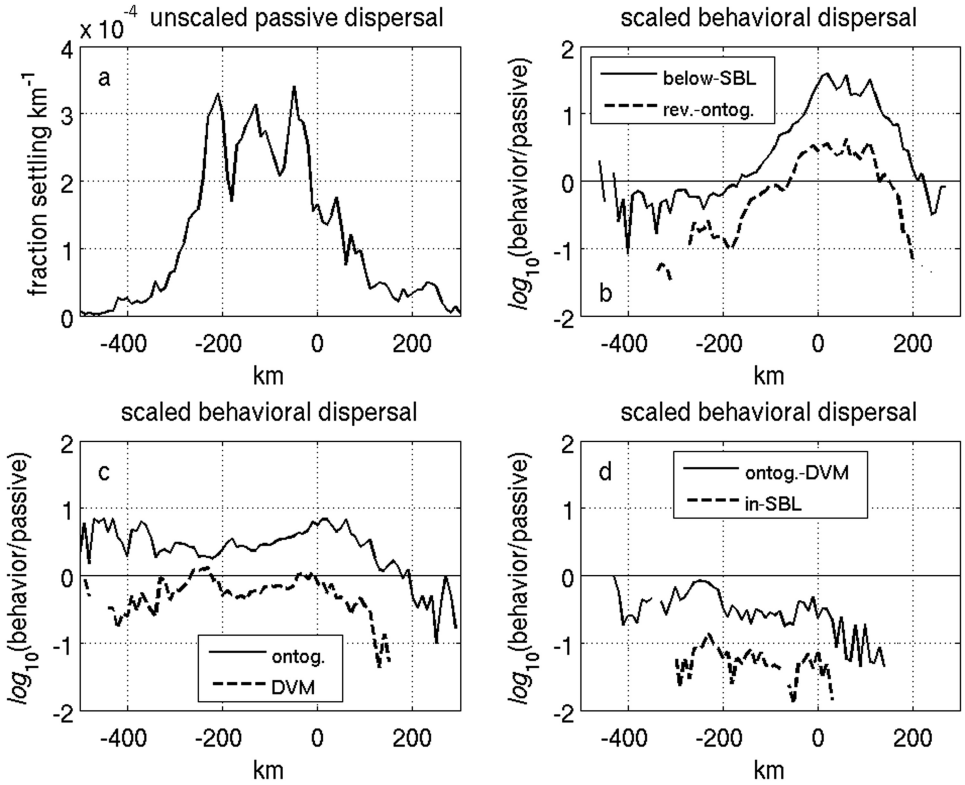

Figure 10. Spring dispersal (i.e., settlement) from the Bodega Bay release cell as a function of alongshore displacement, positive poleward. a) Alongshore settlement, $s(x)$, of passive larvae (i.e., the fraction of total larvae released settling per km displaced). In the remaining panels, we use this pattern as a reference state, scale the settlement of the non-passive behaviors by this function, and plot the ratio formed using a log_{10} scale (i.e., $log_{10}(s_{\text{behavior}}/s_{\text{passive}})$). With this scaling, values above and below the x-axis represent increased and reduced settlement relative to the passive case, respectively. Missing values indicate zero settlement. For settlement only, positive alongshore was defined as 327°, approximately northwestward along the general strike of the central California coastline (Figure 2). b) below-SBL (solid) and reverse-ontogenetic (dashed). c) ontogenetic (solid) and DVM (dashed). d) ontogenetic-DVM (solid) and in-SBL (dashed).

(Figure 10a). The three primary peaks represent, from left to right, settlement in and around the southern Monterey Bay area (the Monterey Peninsula and Pt. Sur), the southern Gulf of the Farallones (Pt. Ano Nuevo and Pigeon Pt.) and the Pt. Reyes area. In the remaining panels, we use this pattern as a reference state, and scale the settlement of the non-passive behaviors by this function.

Settlement is everywhere less than the passive case for both in-SBL and ontogenetic-DVM larvae (Figure 10d), and the relative performance of all the remaining behaviors

depends on alongshore distance. For example, settlement for the below-SBL behavior is greater than the passive case within ∼±200 km of release and is less elsewhere (Figure 10b). The northern limit of this increased settlement ($x = 200$) lies just north of Pt. Arena, as suggested by Figure 7a. Absolute (unscaled) settlement for this case (not shown) displayed a peak immediately at the release site and decreased by 80% within ∼±100 km of Bodega Bay. The reverse-ontogenetic behavior shows a similar but less pronounced pattern to the below-SBL case; the area of increased settlement is limited to ∼-75 to 125 km from the source (Figure 10b). Reverse-ontogenetic larvae experienced increased local settlement, but reduced southward dispersal relative to the passive behavior, with the net result of nearly identical settlement strengths for these two cases. For the ontogenetic behavior, settlement is much greater than the passive case over most of central California, from Pt. Arena ($x = 200$ km) southward (Figure 10c). Ontogenetic settlement is also greater than the below-SBL case at locations south of the Gulf of the Farallones ($x < -200$ km). For the DVM behavior, settlement is almost everywhere slightly less than the passive case, with the exception of the immediate release site and the southern Monterey Bay area (Figure 10d).

b. Dispersal and population connectivity throughout CCS

Connectivity matrices allow the identification of distinct source-sink dispersal relationships amongst potential nearshore sub-populations throughout the CCS. Here we present several connectivity matrices that both demonstrate the broad importance of behavior and highlight the differing impacts of behaviors on different regions (Figures 11, 12 and 13). For the below-SBL behavior (Figure 11b), settlement is generally an order of magnitude or more greater all along the coast compared to the passive case. There is extended and more intense northward dispersal from source cells between Pt. Buchon and Monterey Bay and around the greater Cape Mendocino areas. But settlement is not universally greater for the below-SBL case. For example, southward dispersal from Palos Verdes and cells just south of Pt. Reyes is reduced for the below-SBL larvae relative to the passive case.

In contrast, settlement for in-SBL larvae from source cells in central California is greatly reduced relative to the passive case (Figure 12a). In fact, settlement is almost nonexistent from cells between Pt. Conception and Pt. Arena, except for three small zones or "hotspots" around Pt. Buchon, Monterey Bay, and southern Pt. Reyes. Poleward dispersal from source cells south of Pt. Conception is similar for the passive, in-SBL and DVM cases, however (Figures 11a, 12a,b). The consistent poleward dispersal results from the northern limb of the cyclonic Santa Barbara Channel Eddy (Dong et al. 2009), which is present in the model (Drake et al. 2011) and data (Dong et al. 2009) at near-surface depths (5 to 15 m). The reduction in settlement of in-SBL larvae relative to the passive behavior is relatively minor for southward dispersal from source regions north of Cape Mendocino.

Connectivity for the DVM case clearly shows the spatial variability of the effects of behavior (Figure 12b). Settlement strength over the entire coastline for the DVM behavior is similar to the passive case (Table 5), but subregions of much more intense settlement

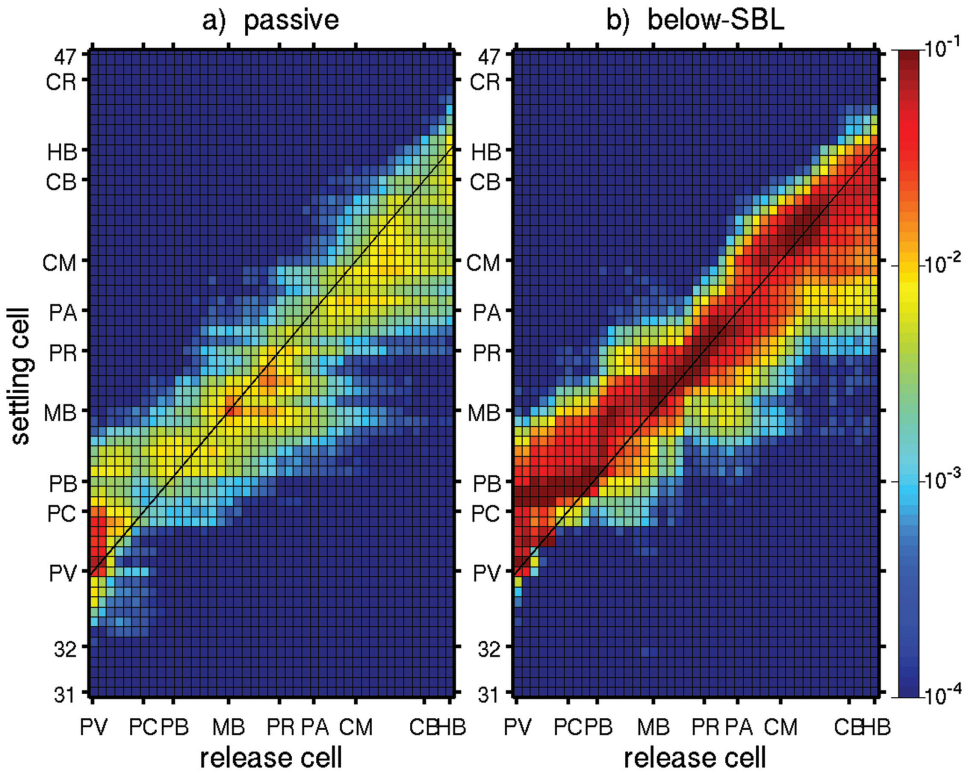

Figure 11. Coastal connectivity given a spring release and 30 to 60 day settlement window for the a) passive and b) below-SBL behaviors, both shown with a log_{10} color scale. We define connectivity as the matrix $C(x, y)$ giving the fraction of larvae released from coastal cell x that settle to coastal cell y. Release locations are given on the x-axis, and settlement locations are on the y-axis. The diagonal line represents local settlement, with color intensity above and below this line indicating northward and southward dispersal, respectively. PV: Palos Verdes; PC: Pt. Conception; PB: Pt. Buchon; MB: Monterey Bay; PR: Pt. Reyes; PA: Pt. Arena; CM: Cape Mendocino; CB: Cape Blanco; HB: Heceta Bank.

are manifest for DVM larvae, specifically Pt. Buchon, Monterey Bay, southern Pt. Reyes (northern Gulf of the Farallones), and an area just north of Cape Mendocino. There is reduced settlement for DVM larvae from source cells between Pt. Reyes and Cape Mendocino.

Ontogenetic and reverse-ontogenetic behaviors also display unique patterns of connectivity (Figure 13). The overall structure of the ontogenetic connectivity all along the coast is similar to the passive case, but more intense. Settlement for ontogenetic larvae is generally less than the below-SBL behavior, but the north-south extent of ontogenetic dispersal is typically broader than the below-SBL case. Relative to passive larvae, there is increased southward dispersal from Bodega Bay to Monterey Bay for the ontogenetic case. Finally,

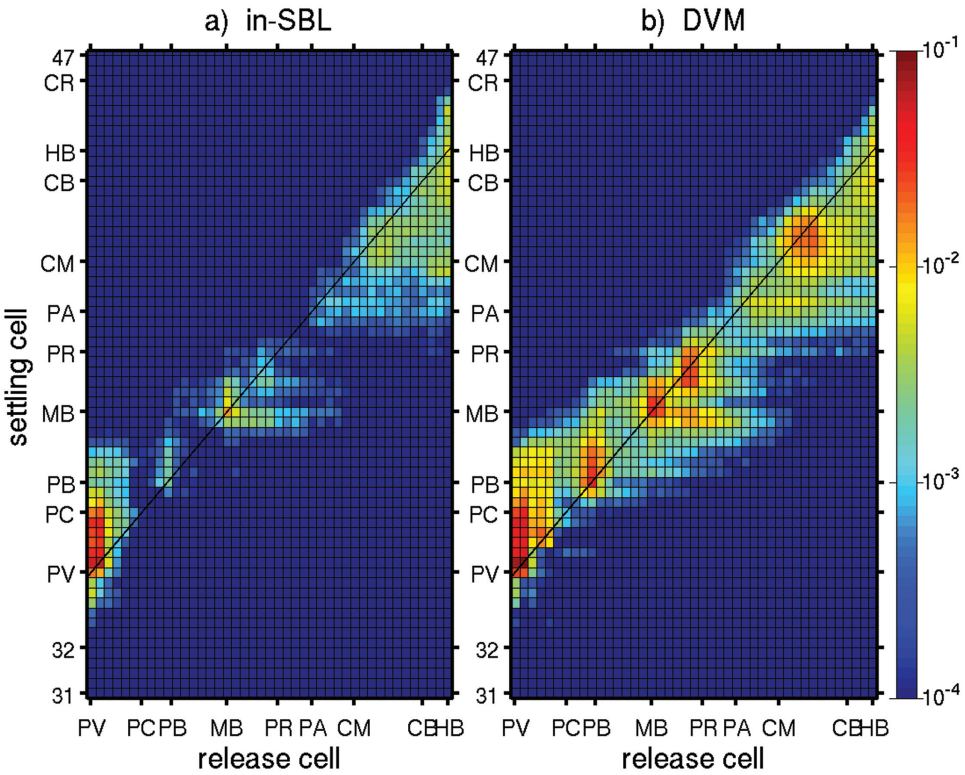

Figure 12. Coastal connectivity given a spring release and 30–60 day settlement window for a) in-SBL and b) DVM behaviors, both shown with a log_{10} color scale. We define connectivity as the matrix $C(x, y)$ giving the fraction of larvae released from coastal cell x that settle to coastal cell y. Release locations are given on the x-axis, and settlement locations are on the y-axis. The diagonal line represents local settlement, with color intensity above and below this line indicating northward and southward dispersal, respectively. PV: Palos Verdes; PC: Pt. Conception; PB: Pt. Buchon; MB: Monterey Bay; PR: Pt. Reyes; PA: Pt. Arena; CM: Cape Mendocino; CB: Cape Blanco; HB: Heceta Bank.

for reverse-ontogenetic larvae, local settlement is greatly increased over most of central California, from Pt. Conception to Pt. Arena, relative to the passive case. And southward dispersal is almost non-existent from source cells south of Monterey Bay for this behavior.

6. Summary of results

The effects of idealized larval vertical swimming behavior on transport and dispersal from nearshore regions of the California Current System (CCS) during spring upwelling conditions were quantified using a numerical simulation. Behaviors that minimized exposure to offshore Ekman transport in the apparent SBL increased nearshore retention by as

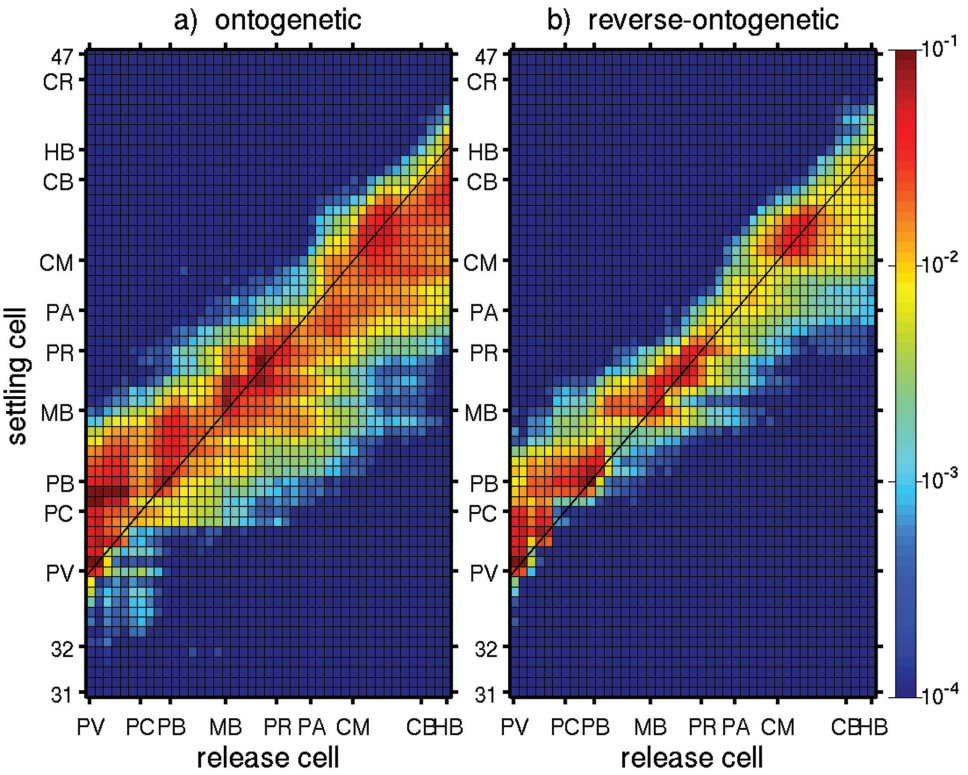

Figure 13. Coastal connectivity given a spring release and 30 to 60 day settlement window for a) ontogenetic and b) reverse-ontogenetic behaviors, both shown with a log_{10} color scale. We define connectivity as the matrix $C(x, y)$ giving the fraction of larvae released from coastal cell x that settle to coastal cell y. Release locations are given on the x-axis, and settlement locations are on the y-axis. The diagonal line represents local settlement, with color intensity above and below this line indicating northward and southward dispersal, respectively. PV: Palos Verdes; PC: Pt. Conception; PB: Pt. Buchon; MB: Monterey Bay; PR: Pt. Reyes; PA: Pt. Arena; CM: Cape Mendocino; CB: Cape Blanco; HB: Heceta Bank.

much as a factor of 500 and settlement by as much as a factor of 140. For larvae released from central California, remaining in the SBL for the initial nine days of larval development and then descending to 30 m resulted in more southward dispersal, while avoiding the layer at all times encouraged local settlement. The impact of behavior varied with source region of the CCS.

7. Discussion

Avoiding offshore transport in the SBL throughout development (below-SBL) maintained high larval densities nearshore (Figures 7 and 8), prevented a catastrophic loss of larvae

from the shelf, and allowed for substantial local settlement. These results suggest that if complicating factors such as food availability and predation are reduced or negligible, this behavior should be the preferred strategy of many species. Indeed, larvae of a large majority of nearshore invertebrate species develop below the SBL to complete development on the inner shelf, and most of them develop <6 km from shore (Morgan et al. 2009a; Shanks and Shearman 2009; Morgan and Fisher 2010). In this nearshore region, offshore Ekman transport due to upwelling is much reduced, and the SBL may be less than 5 m deep (Peterson 1998; Lentz 2001; Kirincich 2005; Nickols et al. 2012). Observed larvae swim against the vertical flow of upwelled waters to avoid being carried to the surface and are trapped in an onshore flow convergence near the coast (Genin et al. 2005; Shanks and Brink 2005). Our results confirm that remaining below the SBL throughout development enables most larvae to remain close to shore. In addition, our results shed new light on the consequences of this behavior for larval dispersal and population connectivity. For a Bodega Bay release, peak settlement occurred near the release site, and settlement was enhanced over a broad region from 175 km south to 200 km north of the bay, relative to passive larvae (Figure 10).

Fewer species of nearshore invertebrates migrate to the middle of the continental shelf (∼13 km) by initially occurring within the SBL before returning as postlarvae in onshore flow below the SBL (Morgan et al. 2009a; Morgan and Fisher 2010). In our model, an idealized ontogenetic vertical migration enables ∼30% of larvae released to complete development and settle on the inner shelf by descending beneath the deeper SBL offshore (∼20 m) (Table 4 and Figures 7 and 8). As expected, we found that the ontogenetic case increased settlement farther from the release site than species that complete development close to shore due the greater time spent in southward-flowing near-surface currents. Although this behavior also increased settlement as far as ∼150 km to the north relative to the passive case, it increased settlement much farther to the south (∼500 km) (Figure 10).

Other species of nearshore invertebrates complete development close to or on the inner shelf by undertaking a reverse-ontogenetic vertical migration, wherein postlarvae of these species return to shore in the neuston (Shanks 1995b; Morgan et al. 2009a; Morgan and Fisher 2010). Like larvae undertaking an ontogenetic vertical migration, larvae undertaking a reverse-ontogenetic vertical migration were transported farther from shore than larvae that remain beneath the SBL throughout development (Figures 7 and 8). We expected results to be similar for the ontogenetic and reverse-ontogenetic behaviors, because larvae spent the same amount of time in the SBL. However, two to three times as many ontogenetic larvae settled as reverse-ontogenetic (Table 5). The difference results from the opportunity of ontogenetic larvae to return to the inner shelf in subsurface currents immediately before and during their competency period, while the reverse-ontogenetic larvae were near-surface and swept offshore when competent to settle. This comparison highlights the importance of the onset or relative timing of behavior during larval development.

Larvae of many species of nearshore invertebrates from our region undertake DVM (Morgan and Fisher 2010), which has been proposed to enhance nearshore larval retention

(Hobbs et al. 1992; Marta-Almeida et al. 2006; Carr et al. 2008; Domingues et al. 2012). However, this did not occur in our study using an idealized DVM behavior; passive and DVM results were similar. In both cases, larvae were transported offshore and southward in prevailing currents where they eventually settled, and offshore and southward transport was slightly greater for larvae undertaking a DVM than for passive particles (Figures 7 to 9). (Offshore and southward transport was increased even more for larvae undertaking both a diel and ontogenetic vertical migration due to the still greater time spent near the surface (Figure 8)). As a result, settlement was slightly lower throughout most of the region for larvae undertaking DVM, especially north of the Bodega Bay release site. This effect was even more pronounced for larvae undertaking ontogenetic-DVM. The results are site-specific, however. For other release areas such as Monterey Bay, DVM led to greater settlement relative to the passive case (Figures 11 and 12). Our DVM results are roughly consistent with the modeling study of Carr et al. (2008). They found that for a spring release from Monterey Bay, DVM reduced southward offshore transport relative to near-surface, fixed-depth particles, but could not prevent a catastrophic loss of larvae from the bay. Our results indicate DVM greatly increases settlement and retention relative to larvae remaining near-surface (Table 5), but differences relative to the passive case were region-specific. These results contrast with recent simulations of another upwelling region, the western Iberian shelf, where it was found that DVM increased retention over the inner shelf by an order of magnitude relative to passive larvae and was necessary to accurately predict observed larval densities (Marta-Almeida et al. 2006; Peliz et al. 2007; Domingues et al. 2012). It remains to be determined whether larvae timing vertical migrations to diel variation in the winds rather than the diel cycle may better reduce offshore and southward transport. Several species from this region undertake DVMs in the plankton but not in laboratory, raising the possibility that turbulence from diel variation in winds rather than light cue larvae (Miller and Morgan 2013).

Although larvae of the large majority of species complete development on the shelf, larvae of other species initially occur in the SBL and are quickly transported to the outer shelf and into the open ocean (Morgan et al. 2009a; Morgan and Fisher 2010). Our results confirm offshore and alongshore transport of larvae that remain in the SBL (in-SBL case). It is possible that larvae could be entrained in coherent structures that remain near the coast (Halle and Largier 2011; Halle et al. in review), keeping them near natal populations. Postlarvae occur at the surface where they could be transported onshore by winds and both surface and internal waves (Shenker 1988; Hobbs et al. 1992; Shanks 1995b, 2006). Our present results show very low retention for larvae that remain in the SBL throughout development, despite interaction with energetic mesoscale and submesoscale fields. However, the model lacked a sea-breeze, tidal-band and higher frequency waves that may interact with large-scale eddies to confine larvae nearshore.

Of the behaviors investigated, only the below-SBL and ontogenetic cases displayed a maximum in absolute density at the coast (Figure 7). Yet larvae believed to exhibit other behaviors are observed with maximum densities over the inner shelf with far fewer individuals

found offshore (Morgan et al. 2009a; Shanks and Shearman 2009). In the present experiments, larval behaviors were functions of development time or time-of-day, and larvae could not react to their time-varying, oceanographic environment. It is possible that more sophisticated, interactive swimming models could increase the effectiveness of all the behaviors. For example, reverse-ontogenetic larvae could limit the time spent near-surface during intense upwelling periods and increase it during downwelling periods using a cue from the wind-driven turbulence, as suggested for DVM larvae, potentially resulting in significantly more retention and settlement.

Although our model was able to capture the mean structure of the measured cross-shore currents (Figure 4a), sub-surface currents were not well-correlated with measurements in this direction, particularly below the SBL (Table 1). A misrepresentation of fluctuating cross-shore currents at depth could lead to an unrealistic accumulation or export of larvae from the shelf if larvae are timing their vertical migrations based on wind-driven turbulence in the SBL. For example, modeled larvae could descend to mid-depths during a strong upwelling event and not be transported shoreward as expected of real larvae. As previously described, our model did not contain this type of interactive behavior. In addition, along- and cross-shore correlation scales of the observed cross-shore subtidal velocity in the region (Dever 1997b) are relatively short (15 to 30 km), suggesting point-to-point mooring comparisons such as done here may not adequately resolve the spatial variability of the cross-shore current. Due to the climatological nature of our study, we suspect any errors in cross-shore transport more likely result from a misrepresentation of the mean flow. An overly shallow or deep SBL will result in erroneously intense or weak offshore near-surface velocities, and hence larval transport, for a given Ekman transport. At the D90 mooring, our model slightly underestimated the SBL depth, and therefore may be slightly overestimating the overall wind-driven offshore larval transport from Bodega Bay.

Furthermore, the model did not include many oceanographic processes that are potentially important for settlement and could alter results. As previously noted, the diurnal seabreeze cycle may affect cross-shelf and alongshore larval transport and recruitment (Shanks 1995b; Jacinto and Cruz 2007; Morgan et al. 2009c). Semidiurnal tidal cycles, including internal tides and waves, also may transport propagules onshore (Pineda et al. 1994; Shanks 1995b, 2006), but were not modeled. Riverine fresh-water input, which can aggregate larvae through buoyancy fronts (Wing et al. 1998), was also absent. The model employed a minimum water depth of 10 m with a grid spacing of $\sim$3 km and did not resolve the subtidal or intertidal zones where many invertebrate larvae are released. Additionally, some topographic smoothing was required for numerical accuracy that may influence the fidelity of the simulation in this nearshore zone. Lastly, larvae of many species aggregate within 1 m of the surface, especially at night, where the Stokes drift due to wind-driven surface gravity waves not modeled here may help confine larvae or return postlarvae to the coast (Shenker 1988; Shanks 1995b; Morgan et al. 2009c; Morgan and Fishe, 2010; Morgan et al. 2012; Tamura et al. 2012).

In conclusion, for the community of nearshore invertebrate species inhabiting central California, we have provided the first comprehensive model of population connectivity employing both realistic mesoscale currents and behavior-mediated larval transport. Our goal was to quantify how differences in vertical swimming behavior affect larval transport and dispersal throughout the CCS. We believe behaviors are the primary ways larvae of these species realize interspecific differences in cross-shelf retention and settlement during the peak upwelling season in a region of strong, persistent upwelling (Morgan et al. 2009a, b; Morgan and Fisher 2010; Morgan et al. 2012; Miller and Morgan 2013). Indeed, different idealized behaviors resulted in vast differences in retention and dispersal throughout the CCS. In addition, some of these behaviors produce modeled cross-shelf larval distributions qualitatively similar to the best available observations. Large spatial variation in dispersal is a key determinant of the dynamics and structure of adult populations and communities with important consequences for the management of commercial species, design of reserve networks, spread of invasive species, and adaptation or extinction in the midst of global climate change (Morgan 2001; Underwood and Keough 2001; Strathmann et al. 2002; Carr et al. 2003; Morgan and Anastasia 2008). Our model estimates alongshore transport and population connectivity that could not be determined from cross-shelf larval surveys, and it illustrates how different behavior-driven interactions with vertically sheared currents lead to variable alongshore transport and settlement within the CCS.

Acknowledgments. We thank three anonymous reviewers for their helpful comments. This study was supported by a grant to Steven G. Morgan and Christopher A. Edwards from California Sea Grant (R/FISH-218A) and is a contribution of the Bodega Marine Laboratory.

REFERENCES

Antonov, J.I., R.A. Locarnini, T.P. Boyer, A.V. Mishonov and H.E. Garcia. 2006. World Ocean Atlas 2005, Volume 2: Salinity, S. Levitus, ed., NOAA Atlas NESDIS 62, U.S. Government Printing Office, 182 pp.

Batchelder, H.P., C.A. Edwards and T.M. Powell. 2002. Individual-based models of copepod populations in coastal upwelling regions: implications of physiologically and environmentally influenced diel vertical migration on demographic success and nearshore retention. Prog. in Oceanogr., *53(2–4)*, 307–333.

Benoit-Bird, K. J. 2009. Dynamic 3-dimensional structure of thin zooplankton layers is impacted by foraging fish. Mar. Ecol. Prog. Ser., *396*, 61–76.

Caley, M.J., M.H. Carr, M.A. Hixon, T.P. Hughes, G.P. Jones and B.A. Menge. 1996. Recruitment and the local dynamics of open marine populations. Ann. Rev. Ecol. Syst., *27*, 477–500.

Carr, M.H., J.E. Neigel, J.A. Estes, S. Andelman, R.R. Warner and J.L. Largier. 2003. Comparing marine and terrestrial ecosystems: implications for the design of coastal marine reserves. Ecol. Appl., *13(1)* Supplement: S90–S107.

Carr, S.D., X.J. Capet, J.C. McWilliams, J.T. Pennington and F.P. Chavez. 2008. The influence of diel vertical migration on zooplankton transport and recruitment in an upwelling region: estimates from a coupled behavioral-physical model. Fish. Oceanogr., *17*(1), 1–15.

Cervantes, B.T.K. and J. S. Allen. 2006. Numerical model simulations of continental shelf flows off northern California. Deep-Sea Res. Pt. II, *53*, 2956–2984.

Checkley, D.M., Jr. and J.A. Barth. 2009. Patterns and processes in the California Current System. Prog. in Oceanogr., *83(1–4)*, 49–64.

Cheriton, O.M., M.A. McManus, D.V. Holliday, C.F. Greenlaw, P.L. Donaghay and T.J. Cowles. 2007. Effects of mesoscale physical processes of thin zooplankton layers at four sites along the west coast of the U.S. Estuaries and Coasts, *30*(4), 575–590.

Collier, M.A. and P.J. Durack. 2006. The CSIRO netCDF version of the NODC World Ocean Atlas 2005, CSIRO Marine and Atmospheric Research Paper 015.

Cowen, R.K., C.B. Paris, D.B. Olson and J.L. Fortuna. 2003. The role of long distance dispersal versus local retention in replenishing marine populations. J. Gulf Carib. Sci., *14*, 129–137.

Cowen, R.K. and S. Sponaugle. 2009. Larval dispersal and marine population connectivity. Annu. Rev. Mar. Sci., *1*, 443–466, doi: 10.1146/annurev.marine.010908.163757.

Davis, R.E. 1985. Drifter observations of coastal surface currents during CODE: the statistical and dynamical views. J. Geophys. Res., *90*(C3), 4756–4772.

Davis, R.E. 1991. Observing the general circulation with floats. Deep Sea Res., *38*(S1), S531–S571.

Dever, E.P. 1997a. Wind-forced cross-shelf circulation on the northern California shelf. J. Phys. Oceanogr., *27*, 1566–1580.

Dever, E.P. 1997b. Subtidal velocity correlation scales on the northern California shelf. J. Geophys. Res., *102*(C4), 8555–8571.

Dever, E.P., C.E. Dorman and J.L. Largier. 2006. Surface boundary-layer variability off northern California, USA, during upwelling. Deep-Sea Res. II, *53(25–26)*, 2887–2905.

Domingues, C.P., R. Nolasco, J. Dubert and H. Queiroga. 2012. Model-derived dispersal pathways from multiple source populations explain variability of invertebrate larval supply. Plos. One, *7*(4), e35794. doi.:10.1371/journal.pone.0035694.

Dong, C., E.Y. Idica and J.C. McWilliams. 2009. Circulation and multiple-scale variability in the Southern California Bight. Prog. Oceanogr., *82*, 168–190.

Drake, P.T., M.A. McManus and C.D. Storlazzi. 2005. Local wind forcing of the Monterey Bay area inner shelf. Cont. Shelf Res., *25*, 397–417.

Drake, P.T., C.A. Edwards and J.A. Barth. 2011. Dispersion and connectivity estimates along the U.S. west coast from a realistic numerical model. J. Mar. Res., *69(1)* 1–37.

Dudas, S.E., B.A. Grantham, A.R. Kirincich, B.A. Menge, J. Lubchenco and J.A. Barth. 2008. Current reversals as determinants of intertidal recruitment on the central Oregon coast. ICES J. of Mar. Sci., *66*, 396–407.

Emery, W.J. and R. E. Thomson. 1997. Data Analysis Methods in Physical Oceanography. Elsevier, 634 pp.

Farrell, T.M., D. Bracher and J. Roughgarden. 1991. Cross-shelf transport causes recruitment to intertidal populations in central California. Limnol. Oceanogr., *36*(2), 279–288.

García-Reyes, M. and J. L. Largier. 2012. Seasonality of coastal upwelling off central and northern California: New insights, including temporal and spatial variability. J. Geophys. Res., *117*, C03028, doi:10.1029/2011JC007629.

Genin, A., J.S. Jaffe, R. Reef, C. Richter and P.J.S. Franks. 2005. Swimming against the flow: A mechanism of zooplankton aggregation. Science, *308(5723)*, 860–862.

Halle, C.M. and J.L. Largier. 2011. Surface circulation downstream of the Point Arena upwelling center. Cont. Shelf Res., *31(12)*, 1260–1272.

Hansen, D.V. and P.-M. Poulain. 1996. Quality control and interpolation of WOCE-TOGA drifter data. J. Atmos. Ocean. Tech., *13*, 900–909.

Hobbs, R.C. and L.W. Botsford. 1992. Diel vertical migration and timing of metamorphosis of larvae of the Dungeness crab *Cancer magester*. Mar. Biol., *112*, 417–428.

Hobbs, R.C., L.W. Botsford and A. Thomas. 1992. Influence of hydrographic conditions and wind forcing on the distribution and abundance of dungeness crab, *Cancer magister*, larvae. Can. J. Fish. Aquat. Sci., *49(7)*, 1379–1388.

Hodur, R.M. 1997. The Naval Research Laboratory's Coupled Ocean/Atmosphere Mesoscale Prediction System (COAMPS). Mon. Weather Rev., *125*, 1414–1430.

Hodur, R.M., J. Pullen, J. Cummings, X. Hong, J.D. Doyle, P. Martin and M.A. Rennick. 2002. The Coupled Ocean/Atmosphere Mesoscale Prediction System (COAMPS). Oceanography, *15(1)* 88–98.

Iles, A.C., T.C. Gouhier, B.A. Menge, J.S. Stewart, A.J. Haupt and M.C. Lynch. 2012. Climate-driven trends and ecological implications of event-scale upwelling in the California Current System. Global Change Biol., *18(2)*, 783–796, doi: 10.1111/j.1365-2486.2011.02567.x.

Jacinto, D. and T. Cruz. 2008. Tidal settlement of the intertidal barnacles *Chthamalus* spp. in SW Portugal: interaction between diel and semi-lunar cycles. Mar. Ecol. Prog. Ser., *366*, 129–135.

Kaplan, D.M., J.L. Largier and L.W. Botsford. 2005. HF radar observations of surface circulation off Bodega Bay (northern California, USA). J. Geophys. Res., *110*(C10), doi:10.1029/2005JC002959.

Kim, S. and J.A. Barth. 2011. Connectivity and larval dispersal along the Oregon coast estimated by numerical simulations, J. Geophys. Res., *116*(6), doi:10.1029/2010JC006741.

Kinlan, B.P. and S.D. Gaines. 2003. Propagule dispersal in marine and terrestrial environments: a community perspective. Ecology, *84*(8), 2007–2020.

Kirincich, A.R., J.A. Barth, B.A. Grantham, B.A. Menge and J. Lubchenco. 2005. Wind-driven inner-shelf circulation off central Oregon during summer. J. Geophys. Res., *110*(C10), doi:10.1029/2004JC002611.

Kosro, P.M. 1987. Structure of the coastal current field off northern California during the Coastal Ocean Dynamics Experiment. J. Geophys. Res., *92*(C2), 1637–1654.

Kundu, P.K. and J.S. Allen. 1976. Some three-dimensional characteristics of low-frequency current fluctuations near the Oregon coast. J. Phys. Oceanogr., *6*, 181–199.

Largier, J.L. 2003. Considerations in estimating larval dispersal distances from oceanographic data. Ecol. Appl., *13*(1), S71–S89.

Largier, J.L., B.A. Magnell and C.D. Winant. 1993. Subtidal circulation over the northern California shelf. J. Geophys. Res., *98*(C10), 18147–18179.

Lentz, S.J. 1987. A description of the 1981 and 1982 spring transitions over the northern California shelf. J. Geophys. Res., *92*(C2), 1545–1567.

Lentz, S.J. 1992. The surface boundary layer in coastal upwelling regions. J. Phys. Oceanogr., *22*, 1517–1539.

Lentz, S.J. 2001. The influence of stratification on the wind–driven cross-shelf circulation over the North Carolina shelf. J. Phys. Oceanogr., *31*, 2749–2760.

Locarnini, R.A., A.V. Mishonov, J.I. Antonov, T.P. Boyer and H.E. Garcia. 2006. World Ocean Atlas 2005, Volume 1: Temperature, S. Levitus, ed., NOAA Atlas NESDIS 61, U.S. Government Printing Office, 182 pp.

Marta-Almeida, M., J. Dubert, Á. Peliz and H. Queiroga. 2006. Influence of vertical migration pattern on retention of crab larvae in a seasonal upwelling system. Mar. Ecol. Prog. Ser., *307*, 1–19.

McManus, M.A., O.M. Cheriton, P.T. Drake, D.V. Holliday, C.D. Storlazzi, P.L. Donaghay and C.F. Greenlaw. 2005. Effects of physical processes on structure and transport of thin zooplankton layers in the coastal ocean. Mar. Ecol. Prog. Ser., *301*, 199–215.

Metaxas, A. 2001. Behavior in flow: Perspectives on the distribution and dispersion of meroplanktonic larvae in the water column. Can. J. Fish. Aquat. Sci., *58*, 86–98.

Metaxas, A. and M. Saunders. 2009. Quantifying the "bio-" components in biological models of larval transport in marine benthic invertebrates: Advances and pitfalls. Biol. Bull., *216*, 257–272.

Miller, S.H. and S.G. Morgan. 2013. Interspecific differences in depth preference regulate larval transport in an upwelling regime. Mar. Ecol. Prog. Ser., *476*, 301–306.

Mitari, S.D., A. Siegel, J.R. Watson, C. Dong and J.C. McWilliams. 2009. Quantifying connectivity in the coastal ocean with application to the Southern California Bight. J. Geophys. Res., *114*(C10026), doi:10.1029/2008JC005166.

Morgan, S.G. 2001. The larval ecology of marine communities, *in* Community Ecology, M.D. Bertness, S.D. Gaines and M. E. Hay, eds., Sinauer, 159–181.

Morgan, S.G. and J.R. Anastasia. 2008. A behavioral tradeoff conserves transport while increasing the risk of predation across the ranges of marine species. P. Natl. Acad. Sci., *105*, 222–227.

Morgan, S.G. and J.L. Fisher. 2010. Larval behavior regulates nearshore retention and offshore migration in an upwelling shadow and along the open coast. Mar. Ecol. Prog. Ser., *404*, 109-126.

Morgan, S.G., J.L. Fisher, S.H. Miller, S.T. McAfee and J.L. Largier. 2009a. Nearshore larval retention in a region of strong upwelling and recruitment limitation. Ecology, *90*(12), 3489–3502.

Morgan, S.G., J.L. Fisher, A.J. Mace, L. Akins, A.M. Slaughter and S.M. Bollens. 2009b. Cross-shelf distributions and recruitment of crab postlarvae in a region of strong upwelling. Mar. Ecol. Prog. Ser., *380*, 173–185.

Morgan, S.G., J.L. Fisherm and A. J. Mace. 2009c. Larval recruitment in a region of strong, persistent upwelling and recruitment limitation. Mar. Ecol. Prog. Ser. *394*, 79–99.

Morgan, S.G., J.L. Fisher and J.L. Largier. 2011. Laval retention, entrainment and accumulation in the lee of a small headland: recruitment hotspots along windy coasts. Limnol. and Oceanogr., *56*, 161–178.

Morgan, S.G., J.L. Fisher, S.T. McAfee, J.L Largier and C.M. Halle. 2012. Limited recruitment during relaxation events: larval advection and behavior in an upwelling system. Limnol. Oceanogr., 57, 457–470.

Nickols, K.J., B. Gaylord and J.L. Largier. 2012. The coastal boundary layer: Predictable current structure decreases alongshore transport and alters scales of dispersal. Mar. Ecol. Prog. Ser., *464*, 17–35

Naylor, E. 2006. Orientation and navigation in coastal and estuarine zooplankton. Mar. Freshw. Behav. Phys., *39*(1), 13–24.

North, E.W., A. Gallego, P. Petitgas and others. 2009. Manual of recommended practices for modeling physical-biological interactions during fish early life. ICES Cooperative Research Report, 295, International Council for the Exploration of the Sea, Copenhagen, 118 pp.

Paris, C.B. and R.K. Cowen. 2004. Direct evidence of a biophysical retention mechanism for coral reef fish larvae. Limnol. Oceanogr., *49*(6), 1964–1979.

Parrish, R.H., C.S. Nelson and A. Bakun. 1981. Transport mechanisms and reproductive success of fishes in the California Current. Biolog. Oceanogr., *1*(2),175–203.

Peliz, A., P. Marchesiello, J. Dubert, M. Marta-Almeida, C. Roy and H. Queiroga. 2007. A study of crab larvae on the Western Iberian Shelf: Physical processes. J. Marine Syst., *68*, 215–236.

Petersen, C.H., P.T. Drake, C.A. Edwards and S. Ralston. 2010. A numerical study of inferred rockfish (*Sebastes* spp.) larval dispersal along the central California coast. Fish. Oceanogr., *19*(1), 21–41.

Peterson, W. 1998. Life cycle strategies of copepods in coastal upwelling zones. J. Marine Syst., *15*, 313–326.

Pfeiffer-Herbert, A.S., M.A. McManus, P.T. Raimondi, Y. Chao and F. Chai. 2007. Dispersal of barnacle larvae along the central California coast: A modeling study. Limnol. Oceanogr, *52*(4), 1559–1569.

Pineda, J. 1994. Internal tidal bores in the nearshore: Warm-water fronts, seaward gravity currents and the onshore transport of neustonic larvae. J. Mar. Res., *52*, 427–458.

Pineda, J., J.A. Hare and S. Sponaugle. 2007. Larval transport and dispersal in the coastal ocean and consequences for population connectivity. Oceanography, *20*(3), 22–39.

Queiroga, H. and J. Blanton. 2005. Interactions between behaviour and physical forcing in the control of horizontal transport of decapod Crustacean larvae. Adv. Mar. Biol., *47*, 107–214.

Rosenfeld, L., I. Shulman, M. Cook, J. Paduan and L. Shulman. 2009. Methodology for a regional tidal model evaluation, with application to central California. Deep-Sea Res. II, *56*, 199–218.

Roughan, M., N. Garfield, J. Largier, E. Dever, C. Dorman, D. Peterson and J. Dorman. 2006. Transport and retention in an upwelling region: The role of across-shelf structure. Deep-Sea Res. II, *53*, 2931–2955.

Roughgarden, J., S. Gaines and H. Possingham. 1988. Recruitment Dynamics in Complex Life Cycles. Science, *241*, 1460–1466.

Shanks, A.L. 1985. Behavioral basis of internal-wave-induced shoreward transport of megalopae of the crab *Pachygrapsus crassipes.* Mar. Ecol. Prog. Ser., *24*, 289–295.

Shanks, A.L. 1986. Vertical migration and cross-shelf dispersal of larval *Cancer* spp. and *Randallia ornata* (Crustacea: Brachyura) off the coast of southern California. Mar. Biol., *92*, 189–199.

Shanks, A.L. 1995a. Oriented swimming by megalopae of several eastern North Pacific crab species and its potential role in their onshore migration. J. Exp. Mar. Biol. Ecol., *186*, 1–16.

Shanks, A.L. 1995b. Mechanisms of cross-shelf dispersal of larval invertebrates and fishes, *in* Ecology of Marine Invertebrate Larvae, L. McEdward, ed., CRC, 323–367.

Shanks, A.L. 2006. Mechanisms of cross-shelf transport of crab megalopae inferred from a time series of daily abundance. Mar. Biol., *148*, 1383–1398.

Shanks, A.L. and L. Brink. 2005. Upwelling, downwelling, and cross-shelf transport of bivalve larvae: A test of a hypothesis. Mar. Ecol. Prog. Ser., *302*, 1–12.

Shanks, A.L. and G.L. Eckert. 2005. Population persistence of California Current fishes and benthic crustaceans: a marine drift paradox. Ecol. Monogr., *75*(4), 505–524.

Shanks, A.L. and R.K. Shearman. 2009. Paradigm lost? Cross-shelf distributions of intertidal invertebrate larvae are unaffected by upwelling or downwelling. Mar. Ecol. Prog. Ser., *385*, 189–204.

Shenker, J.M. 1988. Oceanographic associations of neustonic larval and juvenile fishes and Dungeness crab megalopae off Oregon. Fishery Bulletin, *86*, 299–317.

Shchepetkin, A.F. and J.C. McWilliams. 2005. The regional oceanic modeling system (ROMS): a split-explicit, free-surface, topography-following-coordinate oceanic model. Ocean Model., *9*(4), 347–404.

Song, Y.T. and D.B. Haidvogel. 1994. A semi-implicit ocean circulation model using a generalized topography-following coordinate system. J. Comput. Phys, *115*, 228–244.

Strathmann, R., T. Hughes, A. Kuris, K. Lindeman, S. Morgan, J. Pandolfi and R. Warner. 2002. Evolution of local recruitment and its consequences for marine populations. B. Mar. Sci., *70*, 377–396.

Strub, P.T., J.S. Allen, A. Huyer and R.L. Smith. 1987. Seasonal cycles of currents, temperatures, winds, and sea level over the northeast Pacific continental shelf: 35°N to 48°N. J. Geophys. Res., *92*(C2), 1507–1526.

Strub, P.T., P.M. Kosro and A. Huyer. 1991. The nature of the cold filaments in the California Current System. J. Geophys. Res., *96*(C8), 14743–14768.

Swenson, M.S. and P.P. Niiler. 1996. Statistical analysis of the surface circulation of the California Current. J. Geophys. Res., *101*(C10), 22631–22645.

Tamura, H., Y. Miyazawa and L.-Y. Oey. 2012. The Stokes drift and wave induced-mass flux in the North Pacific. J. Geophys. Res., *117*(C08021), doi:10.1029/2012JC008113.

Thorson, G. 1950. Reproductive and larval ecology of marine bottom invertebrates. Biol. Rev., *25*, 1–45.

Umlauf, L. and H. Burchard. 2003. A generic length-scale equation for geophysical turbulence models. J. Mar. Res., *61*, 235–265.

Underwood, A.J. and M.J. Keough. 2001. Supply-side ecology: the nature and consequences of variations in recruitment of intertidal organisms, *in* Marine Community Ecology, M. D. Bertness, S. D. Gaines and M. E. Hay, eds., Sinauer, 183–200.

Wang, X., Y. Chao, C. Dong, J. Farrara, Z. Li, J.C. McWilliams, J. Paduan and L. Rosenfeld. 2009. Modeling tides in Monterey Bay, California. Deep-Sea Res. II, *56*, 219–231.

Warner, J.C., C.R. Sherwood, H.G. Arango and R.P. Signell. 2005. Performance of four turbulence closure models implemented using a generic length scale method. Ocean Model., *8*, 81–113.

Warner, R.R., S.E. Swearer and J.E. Caselle. 2000. Larval accumulation and retention: implications for the design of marine reserves and essential fish habitat. B. Mar. Sci., *66*(3), 821–830.

Winant, C.D., R.C. Beardsley and R.E. Davis. 1987. Moored wind, temperature, and current observations made during Coastal Ocean Dynamics Experiments 1 and 2 over the northern California continental shelf and upper slope. J. Geophys. Res., *92*(C2), 1569–1604.

Wing, S.R., L.W. Botsford, S.V. Ralston and J.L. Largier. 1998. Meroplanktonic distribution and circulation in a coastal retention zone of the northern California upwelling system. Limnol. and Oceanogr., *43(7)*, 1710–1721.

Wing, S.R., L. Botsford, L.E. Morgan, J.M. Diehl and C.J. Lundquist. 2003. Inter-annual variability in larval supply to populations of three invertebrate taxa in the northern California Current. Estuar. Coast. Shelf Sci., *57*, 859–872.

Received: *Dec. 13, 2013*; revised: *July 23, 2013*.